High Hexane Sorption Capacity of Loosely Crosslinked PDMS Rubbers at Low Temperatures: Macromolecular and Physicochemical Elucidation for VOC Recovery

*M. Inoue[a], E. Ismail[a], S. Samitsu[b], H. Kanoh[c], I. Ichinose[a]**

[a] Research Center for Functional Materials, National Institute for Materials Science, 1−1 Namiki, Tsukuba 305−0044, Japan

[b] Research and Services Division of Materials Data and Integrated System, National Institute for Materials Science, 1−2−1 Sengen, Tsukuba 305−0047, Japan

[c] Graduate School of Science, Chiba University, 1−33 Yayoi-cho, Inage, Chiba 263−8522, Japan

KEYWORDS: soft PDMS, elastic modulus, hexane gas sorption, swelling, low temperature

Corresponding Author

Prof. Dr. Izumi Ichinose – *Research Center for Functional Materials, National Institute for Materials Science, 1−1 Namiki, Tsukuba 305−0044, Japan;* orcid.org/0000-0002-2236-0942; Email: ICHINOSE.Izumi@nims.go.jp

ABSTRACT:

A series of soft polydimethylsiloxane (PDMS) rubbers was obtained by diluting reaction mixtures of a PDMS macromer and a crosslinker with an organic solvent. The degree of swelling of the softest rubber was 600 wt% when immersed in pure hexane at room temperature. From the Flory–Huggins equations, the free energy change for hexane sorption per 1 g rubber was calculated to be −7.4 J g^{-1} and the entropy contribution of the polymer chains was 1.6 J g^{-1} larger than that of the conventional PDMS rubber. The loosely crosslinked PDMS rubber could sorb 776 mg g^{-1} of hexane at 298 K and 606 mg g^{-1} at 195 K. The latter value was 4.4 times larger than that of the conventional PDMS rubber. At a low pressure of 23 Pa, the PDMS rubber sorbed a 3500-fold greater amount of hexane at 195 K, as compared with the value at 298 K. This high sorption amount is because the expansion energy of such soft PDMS rubber is small. The sorption heat of the loosely crosslinked PDMS rubber was 30.3 kJ mol^{-1} when calculated from the Clausius–Clapeyron equation. This value is substantially smaller than that of commercial activated carbon (75 kJ mol^{-1}). Unlike activated carbon, PDMS rubber is insensitive to water and selectively sorbs VOCs even under a saturated humidity. Because of the large swelling potential and small sorption/desorption heat, the loosely crosslinked PDMS rubber will be an indispensable sorbent for the recovery of flammable gasses such as alkane and iso-alkane VOCs in the chemical and oil and gas industries.

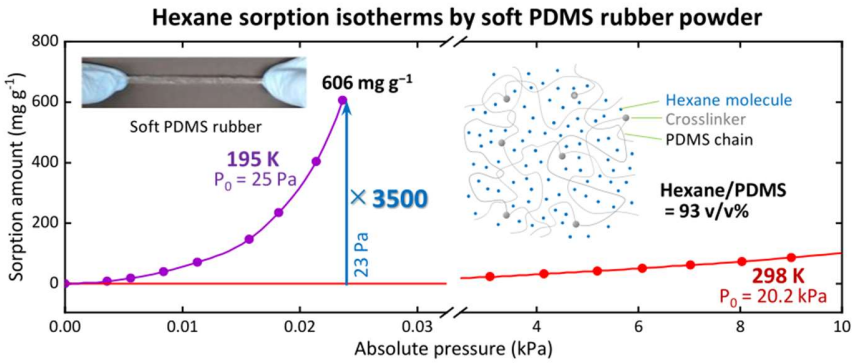

1. Introduction

An energy-efficient technology for the recovery of volatile organic compounds (VOCs) [1,2] is strongly demanded to address the problems of air pollution and global climate change [3,4]. Recovery has been an urgent issue, especially for the chemical, printing, and semiconductor industries, as well as for the development of oil, gas, and other fossil fuels. The present major recovery methods are cryogenic condensation, pressure-swing adsorption, liquid-phase absorption, membrane separation, and their combinations [5–8]. Membranes have been used for the separation of VOCs with a high partial pressure. For example, polydimethylsiloxane (PDMS) membranes have been applied for the recovery of VOCs dissolved in water [9]. Strong sorbents are often required for removing trace concentrations of VOCs. Simpsons et al. designed a Friedel–Crafts-modified polystyrene with improved sorption ability comparable to that of activated carbon (AC). Their sorbent was insensitive to humidity and easy to regenerate [10].

Adsorbents such as AC and silica gel efficiently adsorb VOCs; however, the desorption of the VOCs (regeneration of adsorbents) requires a large amount of energy. In general, AC is regenerated at temperatures greater than 300 °C under vacuum conditions. By contrast, regeneration of polymeric sorbents, such as crosslinked polystyrene and acrylic resin, carried out in vacuum at temperatures less than 100 °C in order to prevent the deterioration. These sorbents are also critical for removing VOCs with a low vapor pressure [11]. Recently, porous organic crystals have attracted attention because of their excellent size-selective sorption properties. For example, Yang et al. reported that a hydrogen-bonded organic framework composed of 3,3′,6,6′-tetracyano-9,9′-bicarbazole showed high C_2H_4/C_2H_6 selectivity [12]. Such strict molecular size/shape separations are expected to reduce the cost of chemical industrial processes substantially, as Sholl et al. have advocated [13]. Interaction between adsorbates and adsorbents such as carbon nanotubes is commonly discussed on the basis of the Lennard–Jones potential. However, in the case of porous polymeric sorbents, sorption behaviors are analyzed by the Brunauer–Emmett–Teller (BET) method or the Kelvin's equation [14,15]. Soft, nonporous polymeric materials also sorb VOCs by swelling, and this behavior is characterized using the χ interaction parameter of the Flory–Huggins theory [16]. However, the sorption energy of polymeric sorbents at room temperature is weak because of the flexibility of the polymer chains. In the case of polymeric sorbents, the sorption of VOCs generally follows Henry's law; that is, the sorption amount increases with increasing VOC vapor pressure. Sanders et al. explained that gas solubility in separation membranes in general depends weakly on the membranes' free volume [17]. This behavior must be true for hard membranes. However, we found that soft PDMS rubbers sorb substantial amounts of gasses and discontinuously swell with increasing vapor pressure, and the gas solubility then increases with the expansion of their volumes even at low temperatures. The last finding has not been reported elsewhere for conventional PDMS rubbers.

PDMS is commonly studied because of its chemical and thermal stabilities as well as its high hydrophobicity resulting from its low surface tension. There are many reports on the separation

performance of organic solvents using PDMS membranes, in which porosity and free volume of the membranes have been studied in detail [18-22]. The highly flexible polymer chains show high diffusion coefficients of various gasses [23,24]. The membranes have often been used for CO_2/N_2 separation, as reported by Liu and coworkers [25]. However, no detailed studies of the sorption behaviors have been conducted through physicochemical measurements such as evaluation of sorption heats and their temperature dependency. This information gap stems from the network structure of PDMS chains drastically changing depending on the sorption amount, and the sorption amount will increase if the network structure is loose.

In the present study, we evaluated the relationship of the elasticity of PDMS rubbers and the sorption ability of hexane from the viewpoints of macromolecular characterization (polymer science) and thermodynamics of the sorption process. PDMS rubbers with different mechanical properties were prepared by diluting PDMS macromers in a good solvent before crosslinking; the polymer chains were fixed as they expanded. We then found that the swelling and sorption properties of soft PDMS rubbers could be improved as much as 400–600% over the swelling and sorption properties of hard ones. This improvement is attributable to a memory effect of the three-dimensional (3D) configuration of the PDMS chains. Many papers on molecular imprinting have been reported for highly crosslinked polymeric materials [26,27]. However, the entanglement-based memory effect in loosely crosslinked PDMS rubbers is, to our best knowledge, the first report in literature.

2. Experimental

2.1. Preparation of loosely crosslinked PDMS rubbers

PDMS rubbers were prepared using a SYLGARD™ 184 kit. Its solution A and solution B are corresponding to PDMS macromer and crosslinker, respectively. The average molecular weights of the PDMS macromer and crosslinker were 57,000 and 3700, as estimated from viscosity measurements (**Figure S1**). The synthesis scheme of the PDMS rubbers is shown in **Figure 1**. This crosslinking reaction is based on hydrosilylation between a vinyl group in the macromer and Si-H group in the crosslinker by means of platinum catalyst. The reaction yields were almost 100 % and polymer elusion was not observed. The crosslinking density is about 0.25 % for all samples, in terms of the ratio of vinyl-modified siloxane units in total siloxane units. A series of PDMS rubbers with different elastic moduli were obtained from 1 g PDMS macromers diluted with 1, 2, 3, 4, or 5 g of hexane containing 0.1 g of crosslinker, followed by curing at 30 ℃. The curing completes in one day for PDMS rubber without hexane dilution and in four days for PDMS rubber diluted with 5 g of hexane. Decane and dodecane were also used as a solvent instead of hexane. All solvents were special-grade products of FUJIFILM Wako Pure Chemical. Curing conditions for diluted reaction mixtures with decane and dodecane were 2 days at 100 ℃. Hexane and decane in solidified reaction mixtures were removed by air/vacuum drying. PDMS rubbers containing dodecane were characterized in their as-prepared state. As shown in **Figure 1**, the polymer chains were

strongly entangled when prepared without a solvent. However, overlap among polymer chains decreased when the chains were crosslinked under the diluted condition with a solvent. The former yielded a hard gel, whereas the latter resulted in a soft gel. The names of the samples are denoted with the initial letter of the solvent and the amount. For example, PDMS_h2 is the rubber obtained from 2 g of hexane, 1 g of macromer, and 0.1 g of crosslinker; PDMS_de1.5 and PDMS_do5 are the rubbers prepared with 1.5 g of decane and 5 g of dodecane, respectively, using 1 g of macromer and 0.1 g of crosslinker; and PDMS_0 is the rubber prepared without any solvent.

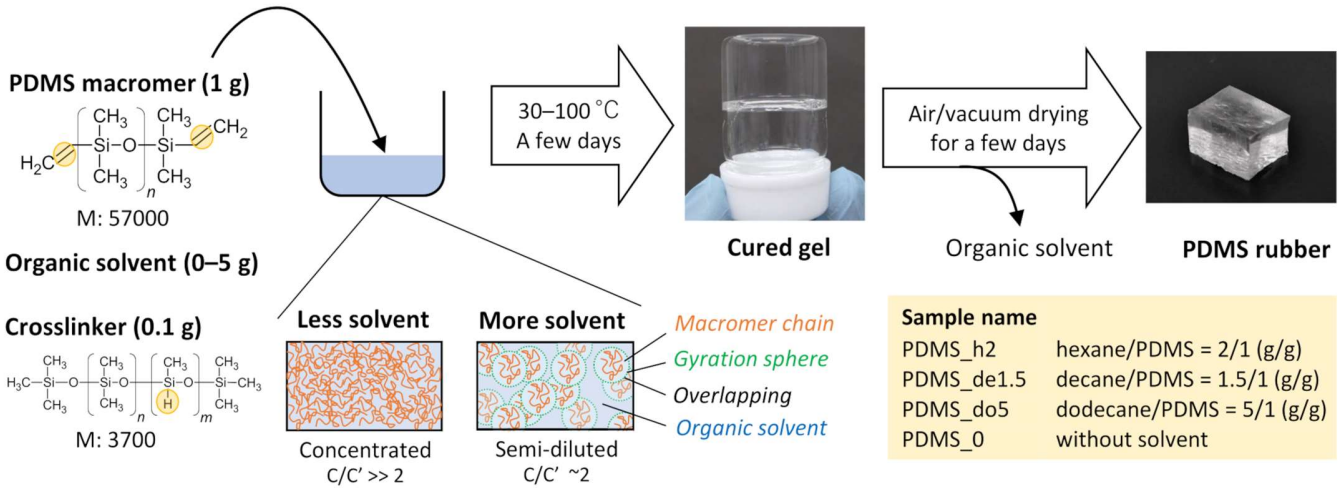

Figure 1. Preparation of PDMS rubbers and a schematic of the PDMS dispersions with different concentrations. The sample names are shown in the yellow box.

2.2. Analysis of thermal and mechanical properties

Viscosity measurements of the polymer solutions were conducted with an AR-G2 (TA Instruments). A tensile tester (Autograph AGS-X, Shimadzu) was used for measuring the elastic moduli of PDMS rubbers. A 2 × 2 × 8 mm^3 sample was pulled at 2.5 mm min^{-1}, and its elastic modulus was calculated when the strain was 3–8%. The elastic modulus in the swollen state was obtained from the samples with a fixed amount of decane sorbed. The experimental error was less than 0.5%. The Poisson's ratio was calculated from the horizontal and vertical deformation observed during a tensile test using a video camera.

Dynamic mechanical analysis (DMA) was conducted using an RSA-G2 (TA Instruments). The storage modulus was obtained in the temperature range from −103 to 25 °C (170–298 K) at a frequency of 1 Hz. The experimental error was less than 1%. Differential scanning calorimetry (DSC) measurements were carried out using a Q2000 (TA Instruments) for dodecane sorbed in PDMS rubbers; samples were analyzed in the temperature range from −90 to 20 °C at a heating rate of +0.5 °C min^{-1}.

2.3. Sorption experiments

The hexane sorption isotherms of PDMS rubbers were obtained for granular samples using a BELSORP-max (MicrotracBEL). The granular samples were prepared by cryogenic grinding (Pulverisette 14, Fritsch) with 80–500 μm sieve rings. The samples were then heated at 50 ℃ for 24 h under vacuum before sorption experiments at 298, 263, and 195 K. Equilibrium criteria in repeated sorption/desorption cycles at 298 and 263 K were set as a pressure deviation of less than 0.3% for 1000 s. At 195 K, the criterion was set as a pressure deviation of less than 0.15% for 4500 s. The error of measured pressures is less than 0.5 %.

3. Results and discussion

3.1. Mechanical properties of PDMS rubbers

The mechanical properties of PDMS rubbers vary substantially with the amount of hexane used in the crosslinking process, that is, the swelling of macromer in crosslinking process largely reduces the elastic modulus of the resultant rubber. **Table 1** shows the elastic moduli of dried PDMS rubbers and their degrees of swelling in hexane. The first sample (PDMS_0) was prepared without using hexane, and the others were prepared using a one- to five-fold weight of hexane relative to the weight of PDMS macromer during the crosslinking process. The elastic modulus of PDMS_0 was 2.0 MPa, and this rubber sorbed 1.0 g g^{-1} of hexane. The elastic modulus of the PDMS_h5 rubber, which had five times more hexane than macromer, decreased to 0.04 MPa, and the rubber sorbed 5.9 g g^{-1} of hexane. The degree of swelling increased in proportion to the amount of hexane used in the crosslinking process. The elastic moduli of these samples exponentially decreased in the series from PDMS_0 to PDMS_h5. In this paper, the rubber with an elastic modulus lower than 0.5 MPa is addressed as loosely crosslinked PDMS rubber.

Table 1. Composition of reaction mixture, degree of overlapping concentration, and material properties of the obtained PDMS rubbers.

Sample	Weight ratio			Hexane / resin (g g^{-1})	Degree of overlapping C/C'	Dry density (g cm^{-1})	†Elastic modulus (MPa)	Degree of swelling in hexane (g g^{-1})
	Macromer	Crosslinker	Hexane					
PDMS_0	1	0.1	0	0	15.6	1.05	2.0	1.0
PDMS_h1	1	0.1	1	0.91	9.6	1.00	0.28	2.2
PDMS_h2	1	0.1	2	1.81	7.0	1.00	0.13	3.5
PDMS_h3	1	0.1	3	2.73	5.5	1.01	0.08	4.2
PDMS_h4	1	0.1	4	3.64	4.5	1.01	0.04	5.3
PDMS_h5	1	0.1	5	4.55	3.8	1.01	0.04	5.9

†The values were obtained for samples in the dried state.

Figure 2 shows the crosslinking structures of the PDMS_0 and PDMS_h5 in reaction mixtures. From the molecular weight of the PDMS macromer (57,000), the contour length of the PDMS chain is calculated to be 126 nm. The average distances between crosslinkers are 4.1 nm for PDMS_0 and 8.1 nm for

PDMS_h5, as determined from the concentration of the crosslinker. Using the results of Arrighi et al. [28] and Higgins et al. [29], we have estimated PDMS macromer gyration radii (r_g) values of 7.3 nm for PDMS_0 and 9.1 nm for PDMS_h5. The former value was obtained from the literature results of small-angle neutron scattering (SANS) experiments, and the latter is based on the swelling effect by a good solvent (refer to the Supporting Information for details). When a five-fold greater amount of hexane relative to the amount of PDMS macromer was added, the volume of the gyration sphere became twice that of PDMS_0. For PDMS_0, the concentration of a certain polymer chain is high at the central part of this sphere, and entanglements with other polymer chains increase at the boundary of this sphere. By contrast, the polymer chains of PDMS_h5 spread out because of the penetration of hexane molecules, and their entanglements are relatively reduced, which results in a very loose crosslinked structure.

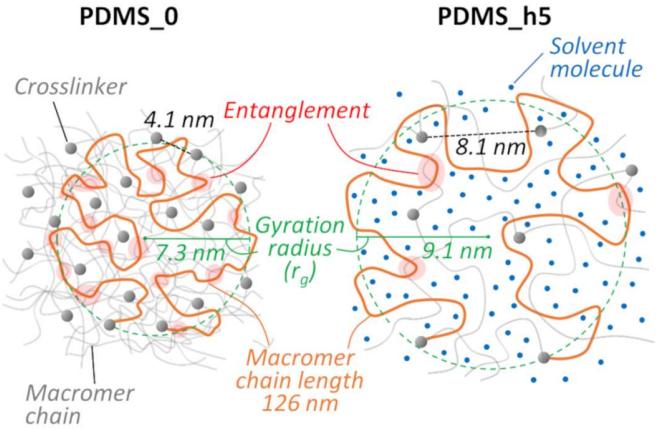

Figure 2. Presumed crosslinking structures of PDMS_0 (left) and PDMS_h5 with solvent molecules (right).

We focused on the degree of overlapping (C/C') to evaluate the extent of entanglements of the PDMS chains diluted in a good solvent. Here, C and C' are the mass concentration of the polymer and the critical concentration, respectively. C' is defined by the following equation [30,31], and the unit is kg m^{-3}.

$$C' = \frac{M/N_A}{(4/3)\pi r_g^3}$$

Here, M is molecular weight (kg mol^{-1}), N_A is Avogadro's number (6.02×10^{23} mol^{-1}), and r_g is the gyration radius (m). At the concentration of C', one polymer molecule is present in a gyration sphere, and overlapping is negligible when $C/C' < 1$, whereas overlapping becomes substantial when $C/C' > 1$. **Table 1** shows the degrees of overlapping calculated from the critical concentration, where r_g^{-2} is expected to change in proportion to the concentration of added hexane [29]. The value for PDMS_0 is

15.6, which means that more than 15 polymer molecules are present within a gyration sphere. The degree of overlapping for PDMS_h5 was 3.8, i.e., one-fourth of the value for PDMS_0. Entanglements still occurred even when hexane was added five-fold relative to the amount of PDMS macromer. The difference in the degrees of overlapping substantially changes both the dry-state elastic moduli and the degrees of swelling.

Figure 3a shows the stress–strain curves of PDMS_h*X* obtained from tensile tests. PDMS_0, which was crosslinked without hexane, exhibited a rupture stress of 3.0 MPa (inset of **Figure 3a**). In sharp contrast, the rupture stress was 0.05 MPa for PDMS_h5, i.e., 1/60 of the value for PDMS_0, even at the same crosslinking density. A further increase in dilution increased the elongation rate and reduced the rupture stress. That is, the entanglement of PDMS chains is reduced. The rupture stress was roughly similar from PDMS_h2 to PDMS_h5, indicating the formation of easily breakable defects within the rubbers. However, the breaking elongation gradually increased to 370%. **Figure 3b** shows pictures of PDMS_0 and

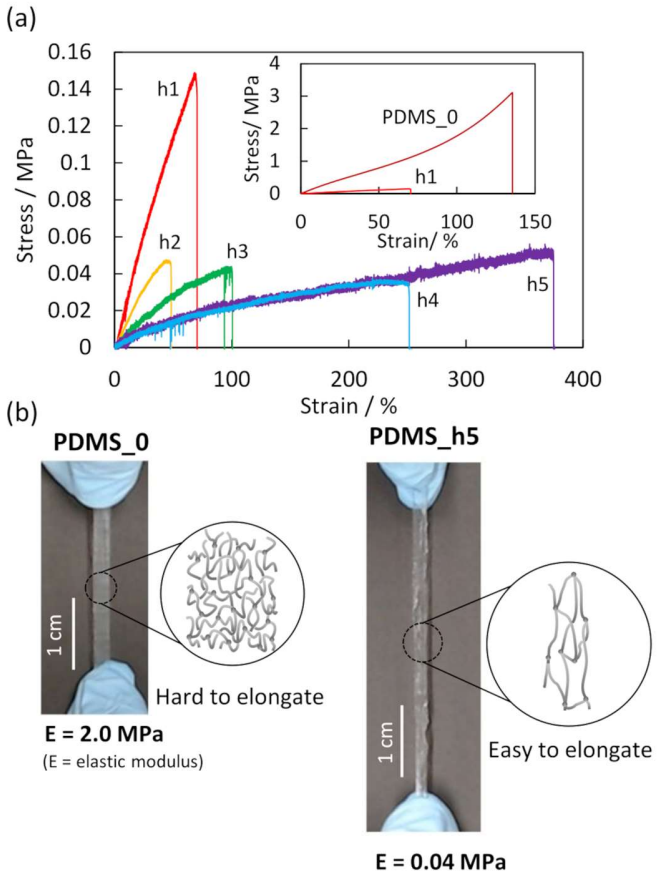

Figure 3. (a) Stress–strain curves for PDMS_h1, PDMS_h2, PDMS_h3, PDMS_h4, and PDMS_h5. The inset is the stress–strain curves for PDMS_0 and PDMS_h1. (b) Pictures of PDMS_0 and PDMS_h5 immediately before breaking and illustrations of their crosslinked polymer chains.

PDMS_h5 immediately before breaking. The latter's elongation rate was slightly less than three times that of the former. However, these samples returned to their original shape when the tensile force was removed, which means that both PDMS_0 and PDMS_h5 exhibited entropic elasticity.

We calculated the elastic moduli (Young's moduli) of these PDMS rubbers in the dried state (**Figure S2**). Interestingly, the elastic moduli of these rubbers decreased exponentially with increasing hexane amount. When the hexane amount was 75–80 wt%, the elastic modulus was 1/50 of that of PDMS_0. In this range, the rubbers became very soft and the data showed some deviations; however, the rubbers were still sufficiently robust to be evaluated by the usual tensile test. The temperature dependence of the elastic moduli in DMA and a tensile test of the PDMS rubber swollen by decane are described in the next section.

3.2. Swelling properties of PDMS rubbers

PDMS rubber sorbs a large amount of hexane. By contrast, the sorption amount of ethanol is very small. Their swelling property is generally explained by crosslinking density of PDMS chains [32–36]. However, our samples have a constant crosslinking density (0.25 %), and only volumes of added hexane are different. **Figure 4a** shows the degree of swelling in hexane–ethanol mixtures plotted against the molar fraction of hexane. The sorption amounts of pure hexane linearly increase with decreasing elastic moduli of the PDMS rubbers, as shown on the right side of **Figure 4a**. Increase of sorption amount is due to the contribution of polymer chain entanglements [37]. The sorption amounts of ethanol are almost zero for all of the samples. At a hexane molar fraction of 0.4, 1 g of PDMS_h5 sorbed 2.2 g of the mixed solvent; when the molar fraction was greater than 0.8, it sorbed 6.0 g of the mixed solvent. The change in sorption amounts did not increase linearly but showed sigmoid-type sorption as a function of the hexane ratio. Kappert et al. reported that crosslinked PDMS membranes sorbed 1.8 g g^{-1} of hexane [38]. Stafie et al. observed the sorption amount increased up to 2.5 g g^{-1} with decreasing the crosslinking density [32]. By contrast, the sorption amounts of PDMS_h2 to PDMS_h5 far exceed these values.

We also evaluated the hexane–ethanol compositions before and after the sorption experiments by measuring the refractive indexes of the immersion solutions (**Figure S3**). In this case, a substantial change in the composition was not observed. That is, hexane was not selectively sorbed at any fraction.

At molar fractions greater than 0.6, the sorption amounts increase in proportion to the hexane amount added during the crosslinking reaction. The 3D configuration of the PDMS chains is memorized during the crosslinking and is maintained even after drying, and the polymer chains return to their original position when the PDMS is immersed in a good solvent. We refer to this phenomenon of polymer chains returning to their original conformation as the "swelling memory effect." The same memory effect was confirmed for hexane gas sorption, as described in the next section. **Figure 4b** shows images of PDMS_0 and PDMS_h5 in the dried state and after being swollen by hexane. PDMS_h5 exhibits a large volume increase because of the memory effect; however, there was no change in shape because of the isotropic

expansion. Both samples are transparent, which means the rubbers are homogenous with respect to refractive index.

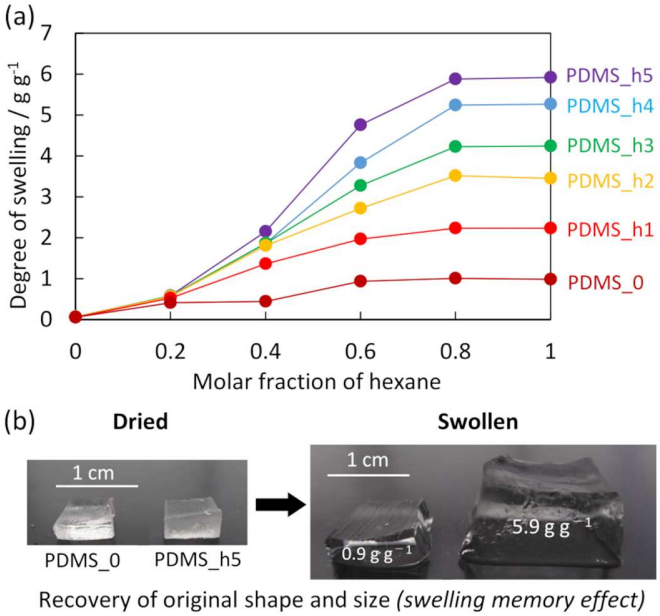

Figure 4. (a) Degree of swelling of PDMS_0, PDMS_h1, PDMS_h2, PDMS_h3, PDMS_h4, and PDMS_h5 rubbers in different hexane–ethanol mixtures. Swelling weights were measured using sealed containers to reduce the experimental error. (b) Volume increase of PDMS_0 and PDMS_h5 by hexane.

Changes in free energy by the mixing of solvent molecules and PDMS chains were estimated using the Flory–Huggins equation [32,33,36,39–47]. This equation is suitable for the thermodynamic evaluation of PDMS and good solvent, especially when the crosslinking density is low. On the other hand, the Flory–Huggins equation cannot predict the distance between crosslinking points, which is usually evaluated by the Flory–Rehner equation [33,34,36,37,46,48–52]. Using the Flory–Huggins equation, the mixing enthalpy change (ΔH_{mix}) was calculated from the molecular weight of the polymer, interaction parameter χ, and the volume fraction of the solvent (refer to the Supporting Information for details). The change in mixing entropy (ΔS_{mix}) was calculated from the volume fraction. The results are shown in **Figure 5a**. The energy plotted on the *y*-axis is normalized against 1 g of PDMS rubber. **Figure 5b** shows the mixing free energy (ΔG_{mix}) calculated from ΔH_{mix} and ΔS_{mix}. In the case of PDMS_0 swollen by hexane at 298 K, ΔH_{mix} and $T\Delta S_{\mathrm{mix}}$ were 8.3 J g^{-1} and 14.2 J g^{-1}, respectively. Note that the former is endothermic (destabilization), whereas the latter is exothermic (stabilization). The ΔG_{mix} for PDMS_h5 was stabilized by 1.6 J g^{-1} compared with that of PDMS_0. This value is corresponding to 23 J mol^{-1} when converted to the per-molar value of sorbed hexane. In case of ethanol sorption to PDMS_h5, the ΔH_{mix}, $T\Delta S_{\mathrm{mix}}$, and ΔG_{mix} were calculated to be 4.7, 8.6, and −3.8 J g^{-1}, respectively. The value of ΔG_{mix} was almost constant for the series from PDMS_0 to PDMS_h5.

Figure 5c shows the fluctuation of PDMS chains and retained hexane molecules in PDMS_0 and PDMS_h5. The retention volume is small for PDMS_0 because the segment number is topologically decreased by entanglement. By contrast, the retention volume for PDMS_h5 is large because of the small degree of entanglement. The increase in the number of states of PDMS chains results in entropic

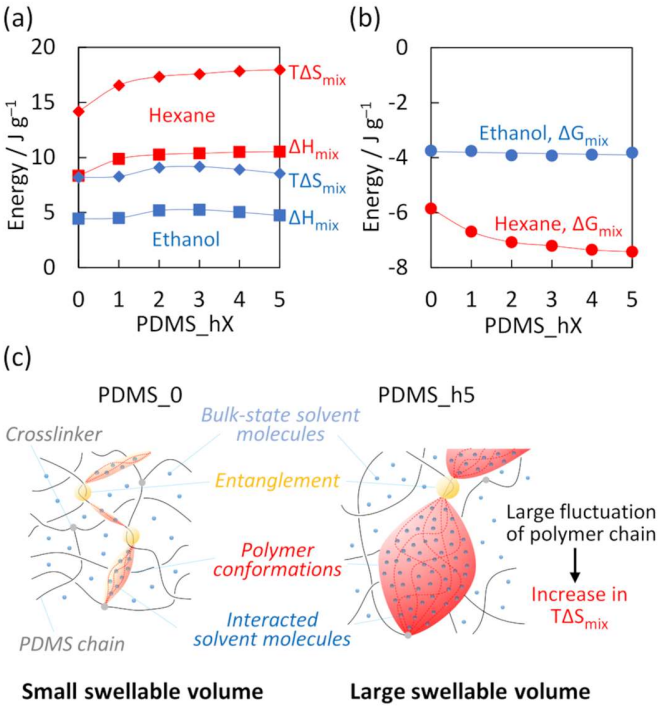

Figure 5. (a) Flory–Huggins' ΔH_{mix} (■) and $T\Delta S_{\mathrm{mix}}$ (♦) values of hexane/PDMS mixtures, and ΔH_{mix} (■) and $T\Delta S_{\mathrm{mix}}$ (♦) values of ethanol–PDMS mixtures at 298 K. (b) ΔG_{mix} of hexane–PDMS (●) and ethanol–PDMS (●) systems. (c) Illustration of the fluctuation of PDMS chains and their retention of hexane.

stabilization, consistent with PDMS_h5 exhibiting the largest $T\Delta S_{\mathrm{mix}}$ value among the investigated samples (**Figure 5a**).

DSC measurements were conducted to evaluate the crystallization behaviors of the polymer and solvent molecules. First, each sample was cooled to −90 °C and the DSC thermogram was acquired at a heating rate of 0.5 °C min^{-1} (**Figure S4**). The thermogram of dry-state PDMS_0 showed a very small peak (3.2 J g^{-1}) at −46.8 °C, which is attributed to the melting of PDMS crystals [53]. **Table 2** shows the results of DSC measurements of sorbed dodecane in PDMS rubbers. Pure dodecane was also measured for reference and exhibited a melting point of −8.6 °C, with a melting enthalpy of 203 J g^{-1} (34.6 kJ mol^{-1}). These values are approximately the same as the reported values [54,55]. In the case of PDMS_do1, a broad endothermic peak was observed at −11.9 °C, along with a comparatively sharp peak of dodecane nanocrystals at −8.6 °C. The former peak is attributed to the dodecane molecules perturbed by flexible

PDMS chains, and the melting enthalpy was twice as large as the latter one. However, a peak or shoulder was not clearly observed near −11.9 °C in the thermogram of PDMS_do3 or PDMS_do5; their thermograms showed only a single peak near the melting peak of pure dodecane. Their FWHM values increased four-fold compared with those of pure dodecane, and the end of the endothermic peak exceeded the melting point of pure dodecane. We speculate that two effects influence the stability of the dodecane nanocrystals: destabilization by the fluctuation of PDMS chains, and stabilization by the network structure of crosslinked PDMS chains. The molar melting enthalpy of dodecane in PDMS rubbers was 10–12% lower than that of pure dodecane.

Table 2. Preparation conditions for PDMS rubbers, along with their dodecane content and DSC data.

Sample	Weight ratio			Dodecane / resin ($g\ g^{-1}$)	Peak position (°C)	†FWHM (°C)	††Melting enthalpy, ΔH_{mel} ($kJ\ mol^{-1}$)	†††Decrease in molar enthalpy ($kJ\ mol^{-1}$)
	Macromer	Crosslinker	Dodecane					
PDMS_do1	1	0.1	1	0.91	−11.9 −8.6	3.2 0.6	20.0 10.3	−4.3
PDMS_do3	1	0.1	3	2.73	−8.6	0.8	31.3	−3.3
PDMS_do5	1	0.1	5	4.55	−8.5	0.7	31.2	−3.4
Dodecane	-	-	-	-	−8.6	0.2	34.6	0

†Full-width of half-maximum. ††Molar enthalpy of dodecane. †††Difference from ΔH_{mel} of pure dodecane.

3.3. Hexane gas sorption

For the hexane gas sorption experiments, we prepared submillimeter-sized PDMS particles. A small particle size is important for achieving a short equilibrium time in the sorption experiments. **Figure 6a** shows the optical images of PDMS_0 and PDMS_de4 obtained by the cryogenic grinding method. By selecting an appropriate mesh size of the sieve rings, we obtained 80 μm powders for hard PDMS_0 rubber and 500 μm powders for soft PDMS_de4 rubber. **Figure 6b** shows the hexane sorption isotherms at 298 K (see also **Figure S5** for the data at 263 K). The relative pressure, P/P_0 (P_0: saturated vapor pressure) is plotted on the abscissa. The sorption amount linearly increased for all samples in the P/P_0 range from 0 to 0.6. The sorption amount at P/P_0 = 0.95 (hexane pressure of 19.2 kPa) was 551 mg g^{-1} (PDMS_0), 641 mg g^{-1} (PDMS_de0.5), and 776 mg g^{-1} (PDMS_de4). The latter values of soft PDMS rubbers are not surprising increases. The adsorption amount of hexane in conventional AC has been reported to be 410 mg g^{-1} at room temperature [11]. This adsorption amount is 55% of the sorption amount of PDMS_de4. In the P/P_0 range lower than 0.6, the hexane sorption obeys Henry's law because the sorbed hexane molecules are isolated among PDMS chains. However, when P/P_0 is high, PDMS chains are partially solvated by hexane molecules. The increase in the sorption amount of soft PDMS rubbers is a phenomenon similar to the increase in the degree of swelling of the soft PDMS rubbers in liquid hexane.

The sorption amounts were 136 mg g^{-1} for PDMS_0 and 606 mg g^{-1} for PDMS_de4 at 195 K and P/P_0 = 0.95 (23.8 Pa) (**Figure 6c**). PDMS rubber usually exhibits a glass-transition temperature (T_g) of ~150 K; thus, both samples should exhibit rubber elasticity. However, the elastic modulus of PDMS_0 was six

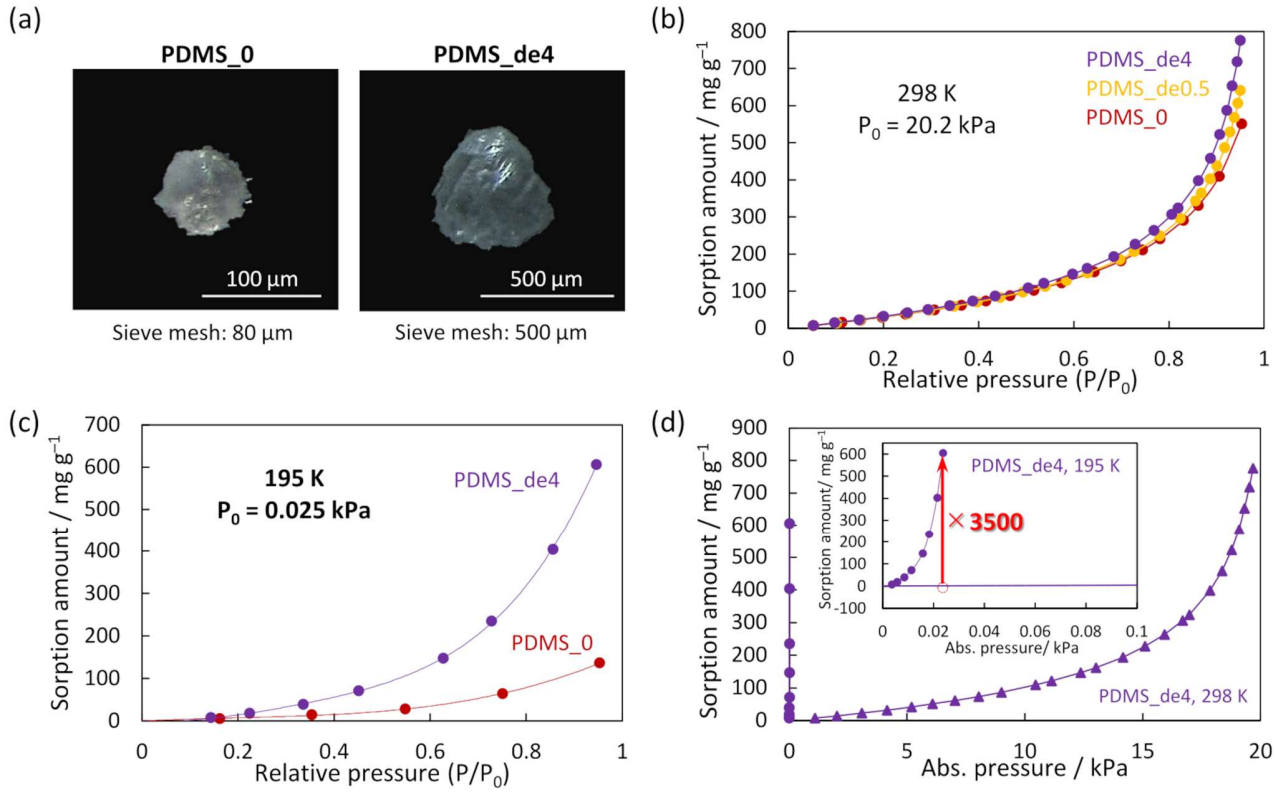

Figure 6. (a) Optical microscope images of PDMS_0 and PDMS_de4 powders prepared by cryogenic grinding. (b) Sorption isotherms of PDMS_0 (●), PDMS_de0.5 (●), and PDMS_de4 (●) at 298 K. (c) Sorption isotherms of PDMS_0 and PDMS_de4 at 195 K. (d) Comparison of the sorption isotherms of PDMS_de4 at 298 and 195 K. The *x*-axis is shown as the absolute pressure. The inset shows magnified plots in the low-pressure range.

times higher than that of PDMS_de4 at 195 K, and this high elasticity led to decrease in sorption amount. **Figure 6d** shows a comparison of the hexane sorption isotherms for PDMS_de4 at 298 K and 195 K, plotted as a function of the absolute pressure. The inset shows isotherms in the low-pressure range. At 298 K and at 1.09 kPa, PDMS_de4 captures 7.60 mg g^{-1} of hexane. In the very low vapor pressure range, the sorption amount obeys Henry's law, and then the hexane sorption at 0.023 kPa is expected to be 0.16 mg g^{-1}. As marked by the red arrow at 23 Pa, the sorption amount at low temperature (195 K) was more than 3500 times greater than the sorption amount at room temperature; that is, PDMS_de4 could sorb large amounts of hexane gas at a vapor pressure of a few tens of pascals (0.01–0.02 mol%, 300–600 ppm). For comparison, the maximum hexane emission regulated by the National Institute for Occupational Safety and Health (NIOSH) is a partial pressure of 1.5 Pa. To meet such a strict limit, trace amounts of hexane need to be removed, for which a strong adsorbent such as AC is indispensable. However, the combined

use of PDMS sorbents could substantially reduce the burden on AC and make it possible to design an environmentally conscious and low-cost VOC recovery system.

Figure 7a shows the sorption heats at 298 and 195 K, as calculated from the Clausius–Clapeyron equation (see Supporting Information). The sorption heats at 298 K for PDMS_0 and PDMS_de4 at the sorption amount of 80 mg g^{-1} were 34.5 and 32.9 kJ mol^{-1}, respectively. These values exceed the condensation heat of hexane of 28.9 kJ mol^{-1}. As the sorption amount decreased from 20 to 0 mg g^{-1}, the sorption heat increased. This trend has often been observed for microporous adsorbents [56], implying the formation of strong sorption sites in PDMS rubbers when small amounts of hexane are sorbed. At the sorption amount of 80 mg g^{-1} at 195 K, the sorption heats for PDMS_0 and PDMS_de4 were 27.4 and 30.3 kJ mol^{-1}, respectively. The condensation heat of hexane increases with decreasing temperature. We calculated the value at 195 K to be 33.6 kJ mol^{-1} using Watson's equation (see Supporting Information) [57]. If compared with this value, the observed sorption heat is much smaller than the condensation heat. At low temperatures, the elastic moduli of PDMS rubbers increase and the rubbers do not readily expand. Some part of the exothermic heat acquired by the sorption of hexane must be consumed for the volume expansion. The heat loss due to the volume expansion was 12 times larger at 195 K than at 298 K, as

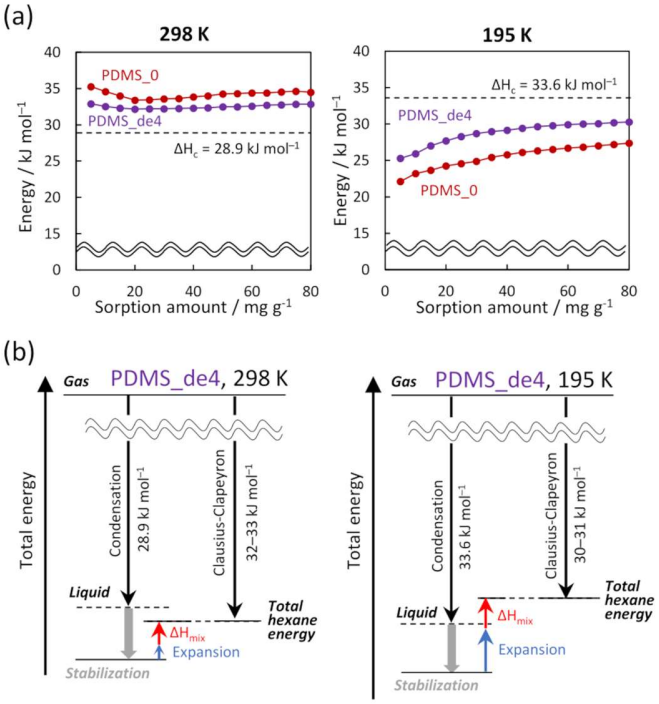

Figure 7. (a) Comparison of the condensation heat (ΔH_c) and the sorption heat (ΔH_{sp}) of PDMS_0 (●) and PDMS_de4 (●) calculated by the Clausius–Clapeyron equation at 298 and 195 K. (b) The energy level diagrams for hexane sorption in PDMS_de4 at 298 and 195 K. ΔH_{mix}: mixing enthalpy change of hexane and PDMS; Expansion: energy loss by volume expansion of PDMS rubber; Stabilization: decrease in total energy mainly due to entropy change.

calculated from the bulk moduli of PDMS_0. Small heat loss was confirmed even for PDMS_de4. These results are discussed later in this section. As evident in **Figure 7a** (right), the sorption heat of PDMS_0 was 2.7–3.7 kJ mol^{-1} smaller than that of PDMS_de4 at 195 K. Interestingly, the sorption heat gradually decreased as the sorption amount decreased from 80 to 0 mg g^{-1}. This trend was opposite to the increase in the sorption heat at 298 K at small sorption amounts between 20 and 0 mg g^{-1}. The beginning of hexane sorption at low temperatures incurs a large energy loss because the rubber's elastic modulus is relatively high.

Figure 7b shows the energy diagrams of hexane sorption into PDMS_de4 at 298 and 195 K. Both temperatures are greater than T_g; thus, the PDMS chains exhibit liquid-like motion. Gaseous hexane is captured by such polymer chains. The total exothermic energy consists of the gas-to-liquid condensation and stabilization energies, mainly because of an increase in the mixing entropy of PDMS chains and hexane molecules. For example, the total energy of the PDMS_de4 system at 298 K decreased by 28.9 kJ mol^{-1} through condensation of hexane and was then further stabilized by the mixing entropy, although the accurate value is unclear. However, some part of the exothermic heat was consumed by the endothermic swelling (expansion) process and the Flory–Huggins' mixing enthalpy (ΔH_{mix}). The sum of exothermic and endothermic heats is consistent with the sorption heat calculated from the Clausius–Clapeyron equation. PDMS rubbers undergo the same exothermic and endothermic processes at 195 K; however, their energy loss due to volume expansion is much larger than that at 298 K because of the high elastic modulus. The sorption heat thus becomes smaller than the condensation heat.

Changes of the elastic moduli and Poisson's ratios of the PDMS rubbers after swelling with small amounts of solvent were evaluated using decane, which exhibits low volatility at room temperature. **Figure 8a** and **8b** show the results. Dried PDMS_0 exhibited an elastic modulus of 2.0 MPa. The moduli decreased quasi-linearly in the initial sorption range (0–8.0 wt%). The modulus for PDMS_0 became 1.1 MPa at 8 wt%. As shown in the inset, the elastic modulus of PDMS_de4 was 0.048 MPa in the absence of decane and became 0.043 MPa when the sorption amount reached 7.8 wt%. **Figure 8b** shows the changes in the Poisson's ratio for PDMS_0 and PDMS_de4 as functions of the sorption amount (see also **Figure S6** for their logarithmic plots). The original value for PDMS_0 was 0.49, and the value became 0.33 when the sorption amount was 6.2 wt%. Although not shown in the figure, the Poisson's ratio was further reduced to 0.30 at 11.5 wt%. By contrast, the Poisson's ratio of PDMS_de4 was 0.48 without decane and 0.38 when the sorption amount was 6.3 wt%. In general, when rubbers are elongated, the horizontal thinning is approximately one-half of the vertical elongation, giving a Poisson's ratio of 0.50. The PDMS_0 and PDMS_de4 have ratios close to 0.50. However, the Poisson's ratio of the PDMS rubbers swollen by decane is far smaller than this value. Presumably, this low ratio is attributable to the solvent molecules in swollen PDMS rubbers readily migrating to the elongated part and preventing the horizontal thinning [58].

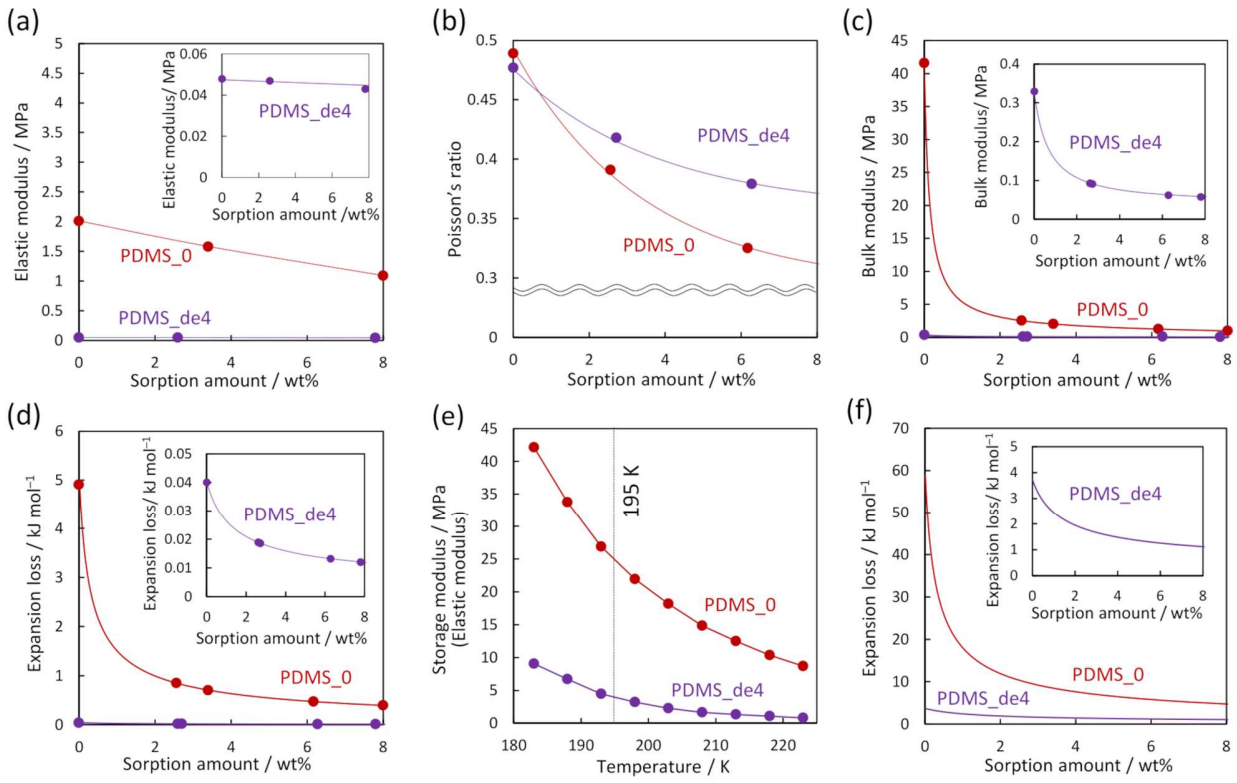

Figure 8. The changes in (a) elastic modulus, (b) Poisson's ratio, (c) bulk modulus, and (d) energy loss due to volume expansion with increasing sorption amount of decane at 298 K. PDMS rubbers: PDMS_0 (●) and PDMS_de4 (●). (e) The relationship between storage modulus and temperature for PDMS_0 and PDMS_de4 in the dried state. (f) Energy loss at 195 K for PDMS_0 and PDMS_de4. The insets in (a), (c), (d), and (f) are the magnified figures for PDMS_de4.

Bulk modulus is important for characterizing swelling phenomena. The value was calculated from elastic modulus and Poisson's ratio using the following equation:

$$K = \frac{E}{3(1-2\nu)}$$

, where E is the elastic modulus (Pa) and ν is the Poisson's ratio. **Figure 8c** shows the decreases of the bulk moduli of PDMS_0 and PDMS_de4 with increasing amount of sorbed decane. The bulk modulus of the former rubber (42 MPa) rapidly decreased with increasing amount of sorbed decane. By contrast, the latter rubber exhibited a small bulk modulus of 0.33 MPa from the beginning; this value is less than 1/130 of the value for PDMS_0. The inset shows enlarged plots of the decrease of the bulk modulus of PDMS_de4. The value became 0.059 MPa when the sorption amount was 7.8 wt%. This modulus is approximately 1/16 of that of PDMS_0 at the same sorption amount. **Figure 8d** shows the changes in energy loss due to volume expansion (see Supporting Information). This value corresponds to the

integration of the bulk moduli in **Figure 8c**, and the unit of the calculated energy is joules per 1 g of dried PDMS rubber, which was converted to kilojoules per 1 mol of decane in **Figure 8d**. The energy loss at the beginning of sorption was 4.9 kJ mol^{-1} for PDMS_0 and 0.04 kJ mol^{-1} for PDMS_de4. The latter was less than 1/120 of that of the former. As shown in the inset, the energy loss for PDMS_de4 at the sorption amount of 7.8 wt% was 0.012 kJ mol^{-1}, or approximately 1/33 of the energy loss for PDMS_0.

The elastic moduli at low temperatures were evaluated by DMA. **Figure 8e** shows the temperature dependency of the storage moduli at 1 Hz. At 195 K, the storage modulus was 24.8 MPa for PDMS_0 and 4.0 MPa for PDMS_de4. **Figure 8f** shows the energy loss due to volume expansion at 195 K. We assumed that the Poisson's ratio did not change in the range 298–195 K. The energy loss for PDMS_0 at the beginning of sorption was then 59 kJ mol^{-1}. By contrast, the energy loss for PDMS_de4 was 3.6 kJ mol^{-1}, which was less than 1/16 of that for PDMS_0.

Notably, the energy loss due to the volume expansion at 195 K is more than ten times greater than that at 298 K. The former value (59 kJ mol^{-1}) far exceeds the condensation heat at 195 K (33.6 kJ mol^{-1}), which is why the sorption of hexane gas at low temperatures is suppressed. However, when the P/P_0 value increases to greater than 0.5, PDMS_0 sorbs a certain amount of hexane because the bulk modulus of this rubber (energy loss due to expansion) decreases with increasing amount of sorbed hexane. Importantly, compared with the condensation heat of hexane, the expansion energy loss of PDMS_de4 (3.6 kJ mol^{-1}) was very small from the beginning. Therefore, this rubber acts as a powerful sorbent for hexane even at very low temperatures.

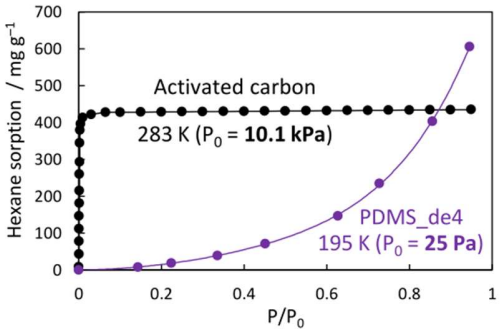

Figure 9. Comparison of hexane sorption isotherms of activated carbon [11] at 283 K and PDMS_de4 at 195 K.

Figure 9 shows sorption isotherms of hexane gas for conventional AC at 283 K and PDMS_de4 at 195 K. The sorption isotherm of PDMS_de4 clearly differs from that of the AC. The maximum sorption amount of PDMS_de4 exceeds that of the AC in the high P/P_0 range. The sorption heat of AC at room temperature has been reported to be 75 kJ mol^{-1}, which is twice the sorption heat of PDMS_de4 (**Table S1**). A high temperature of 882 K or greater is then required for desorption from AC at ambient pressure,

as calculated from Trouton's rule [11]. In sharp contrast, a decrease in pressure is sufficient for PDMS_de4 to desorb hexane even at low temperatures.

Conventional adsorbents such as activated carbon, zeolites, and mesoporous materials have nanometer to subnanometer pores that do not change size during the adsorption of gasses. The adsorption behaviors in these materials are often explained by a micropore filling mechanism or a capillary model. In sharp contrast, polymeric sorbents do not have intrinsic pores and the volume increases with increasing sorption amount. In this case, the sorption of gasses follows Henry's law when the sorption temperature is greater than the T_g of the polymer. The effect of the elastic modulus on the polymer is then substantial. Therefore, the physicochemical sorption behaviors of polymers have not been quantitatively evaluated compared with those of inorganic adsorbents.

Numerous studies on metal–organic frameworks (MOFs) have been reported over the past two decades [**59**]. These materials possess a soft crystalline structure and exhibit unusual adsorption behaviors. Kitagawa et al. reported that porous materials synthesized from copper (II) nitrate, 2,5-dihydroxybenzoic acid, and 4,4′-bipyridine showed a gate opening/closing effect in response to the partial pressure of N_2 [**60**]. Flexible metal–organic microporous materials can strongly adsorb acetylene over CO_2 if the chemical interaction inside the pores is optimized [**61**]. The swelling of rubbers was actively studied in the 1940s. Flory and Rehner reported that the degrees of swelling can be predicted from the crosslinking density of rubber and the χ parameters of the rubber and the solvent [**62**]. In the 1960s, gas sorption and diffusion behaviors of polymer membranes were analyzed using the dual-sorption theory [**63**]. However, substantially high sorption capacity of solvent vapors has not been well studied in either the polymer science or the physicochemistry field. We combined low-temperature gas sorption measurements with static and dynamic mechanical analyses of soft rubbers and evaluated the sorption behavior using the Clausius–Clapeyron equation, estimations of the energy loss due to volume expansion, and the Flory–Huggins' mixing enthalpy. To the best of our knowledge, at low temperatures, this work is the first report of a quantitative evaluation of the sorption behavior of good solvents in soft rubbers. Based on the results reported here, we have examined the separation potential of hexane in our scaled-up bench plant. Woven nylon fabric packages containing PDMS powders were used for separation column to make the handling of PDMS powders much easier and to provide the pathway of hexane gas. The details were explained in Supporting Information (**Figure S7**).

4. Conclusions

PDMS rubbers are expected to be valuable sorbents for hexane recovery. We have explained that PDMS macromers diluted with a large amount of hexane (or decane) can be loosely crosslinked, giving soft rubbers with a reduced degree of entanglement. The elastic modulus exponentially decreased with increasing volume ratio of the solvent. The degree of swelling of soft PDMS rubbers in hexane increased substantially because the 3D configuration of the PDMS chains was memorized during the crosslinking.

Even after drying, the rubber returned to its original structure when immersed in hexane; that is, the swelling memory effect was observed. Enhanced sorption ability was also observed when the PDMS rubbers were exposed to hexane gas. In particular, more than 600 mg g^{-1} of hexane could be captured at low temperatures, even though the partial pressure was low (10–20 Pa). We found that the high sorption amount could be well explained by the substantial decrease in endothermic energy due to the small bulk modulus of soft PDMS rubbers.

If regeneration is not desired, ACs will be the best choice to remove trace amounts of VOCs. However, for the recovery of large amounts of hydrocarbons, the weakly sorbing PDMS rubber becomes important. In fact, the recovery of VOCs at large scale is demanded in various fields, including the chemical industry and the printing and paint industries. The recovery of halogenated solvents in the semiconductor industry is also strongly demanded, as is the removal of greenhouse gasses in the oil and gas industry. We should also emphasize that most of the industrially available adsorbents such as AC and zeolite are not useful under high humidity conditions because of the strong affinity to water. On the other hand, our PDMS rubber sorbs no more than 1 wt% of water, making it absolutely advantageous in the separation process of VOCs even under saturated humidity.

Declaration of Competing Interest

The authors declare that they have no known competing financial interests or personal relationships that could have appeared to influence the work reported in this paper.

Acknowledgements

The authors are grateful for the financial support of Cabinet Office, Government of Japan, Cross-ministerial Moonshot Agriculture, Forestry and Fisheries Research and Development Program, "Technologies for Smart Bio-industry and Agriculture" (No. JPJ009237) and for JST-START program (ST221006UM). The authors also appreciate Mr. R. Ema of National Institute of Technology, Tokyo College for his supports in literature arrangement.

Appendix A. Supporting Information

Supplementary data to this article can be found online at https://~. Viscosities, elastic moduli, refractive indexes, DSC thermograms, sorption isotherms, and Poisson ratios are shown in Figure S1–S6. Calculation or estimation methods of r_g, ΔH_{mix}, ΔS_{mix}, ΔG_{mix}, ΔH_{sp}, ΔH_c, E_{loss}, and comparisons of sorption heats are described.

References

[1] F.I. Khan, A. K. Ghoshal, Removal of volatile organic compounds from polluted air, J. Loss Prev. Process Ind. 13(6) (2000) 527–545. https://doi.org/10.1016/S0950-4230(00)00007-3.

[2] G.R. Parmar, N.N. Rao, Emerging control technologies for volatile organic compounds, Crit. Rev. Environ. Sci. Technol. 39(1) (2008) 41–78. https://doi.org/10.1080/10643380701413658.

[3] M.S. Kamal, S.A. Razzak, M.M. Hossain, Catalytic oxidation of volatile organic compounds (VOCs) – A review, Atmos. Environ. 140 (2016) 117–134. https://doi.org/10.1016/j.atmosenv.2016.05.031.

[4] B.C. McDonald, J.A. de Gouw, J.B. Gilman, S.H. Jathar, A. Akherati, C.D. Cappa, J.L. Jimenez, J. Lee-Taylor, P.L. Hayes, S.A. McKeen, Y.Y. Cui, S.W. Kim, D.R. Gentner, G. Isaacman-VanWertz, A.H. Goldstein, R.A. Harley, G.J. Frost, J.M. Roberts, T.B. Ryerson, M. Trainer, Volatile chemical products emerging as largest petrochemical source of urban organic emissions, Science. 359(6377) (2018) 760–764. https://doi.org/10.1126/science.aaq0524.

[5] P. Dwivedi, V. Gaur, A. Sharma, N. Verma, Comparative study of removal of volatile organic compounds by cryogenic condensation and adsorption by activated carbon fiber, Sep. Purif. Technol. 39(1-2) (2004) 23–37. https://doi.org/10.1016/j.seppur.2003.12.016.

[6] T.C. Bowen, R.D. Noble, J.L. Falconer, Fundamentals and applications of pervaporation through zeolite membranes, J. Memb. Sci. 245(1-2) (2004) 1–33. https://doi.org/10.1016/j.memsci.2004.06.059.

[7] L. Zhu, D. Shen, K.H. Luo, A critical review on VOCs adsorption by different porous materials: Species, mechanisms and modification methods, J. Hazard. Mater. 389 (2020) 122102. https://doi.org/10.1016/j.jhazmat.2020.122102.

[8] Y. Ding, Volatile organic compound liquid recovery by the dead end gas separation membrane process: Theory and process simulation, Ind. Eng. Chem. Res. 58(12) (2019) 5008–5017. https://doi.org/10.1021/acs.iecr.9b00586.

[9] J.G. Wijmans, A.L. Athayde, R. Daniels, J.H. Ly, H.D. Kamaruddin, I. Pinnau, The role of boundary layers in the removal of volatile organic compounds from water by pervaporation, J. Memb. Sci. 109(1) (1996) 135–146. https://doi.org/10.1016/0376-7388(95)00194-8.

[10] E.J. Simpson, W.J. Koros, R.S. Schechter, An emerging class of volatile organic compound sorbents: Friedel−Crafts modified polystyrenes. 2. Performance comparison with commercially-available sorbents and isotherm analysis, Ind. Eng. Chem. Res. 35(12) (1996) 4635–4645. https://doi.org/10.1021/ie9507311.

[11] R. Koyama, F. Tsunoda, I. Ichinose, H. Kanoh, Adsorption properties of methane, ethane, and hexane on mesoporous organic polymers prepared by the flash freezing method, Langmuir. 36(9) (2020) 2184–2190. https://doi.org/10.1021/acs.langmuir.9b03159.

[12] Y. Yang, L. Li, R.B. Lin, Y. Ye, Z. Yao, L. Yang, F. Xiang, S. Chen, Z. Zhang, S. Xiang, B. Chen, Ethylene/ethane separation in a stable hydrogen-bonded organic framework through a gating mechanism, Nat. Chem. 13 (2021) 933–939. https://doi.org/10.1038/s41557-021-00740-z.
[13] David. S. Sholl, Ryan P. Lively., Seven chemical separations to change the world, Nature. 532 (2016) 435–437.
[14] S. Brunauer, P.H. Emmett, E. Teller, Adsorption of gases in multimolecular layers, J. Am. Chem. Soc. 60(2) (1938) 309–319. https://doi.org/10.1021/ja01269a023.
[15] W. Thomson, LX. On the equilibrium of vapour at a curved surface of liquid, London, Edinburgh, Dublin Philos. Mag. J. Sci. 42(282) (1871) 448–452. https://doi.org/10.1080/14786447108640606.
[16] P.J. Flory, Thermodynamics of high polymer solutions, J. Chem. Phys. 10(1) (1942) 51–61. https://doi.org/10.1063/1.1723621.
[17] D.F. Sanders, Z.P. Smith, R. Guo, L.M. Robeson, J.E. McGrath, D.R. Paul, B.D. Freeman, Energy-efficient polymeric gas separation membranes for a sustainable future: A review, Polymer. 54(18) (2013) 4729–4761. https://doi.org/10.1016/j.polymer.2013.05.075
[18] Z. Si, J. Li, L. Ma, D. Cai, S. Li, J. Baeyens, J. Degreve, J. Nie, T. Tan, P. Qin, The Ultrafast and Continuous Fabrication of a Polydimethylsiloxane Membrane by Ultraviolet-Induced Polymerization, Angew. Chem. Int. Ed. Engl. 58(48) (2019) 17175-17179. https://doi.org/10.1002/anie.201908386.
[19] W. Kong, J. Baeyens, P. Qin, H. Zhang, T. Tan, Towards an energy-friendly and cleaner solvent-extraction of vegetable oil, J. Environ. Manage. 217 (2018) 196-206. https://doi.org/10.1016/j.jenvman.2018.03.061.
[20] W. Kong, Q. Miao, P. Qin, J. Baeyens, T. Tan, Environmental and economic assessment of vegetable oil production using membrane separation and vapor recompression, Frontiers of Chemical Science and Engineering 11(2) (2017) 166-176. https://doi.org/10.1007/s11705-017-1616-4.
[21] Z. Si, G. Li, Z. Wang, D. Cai, S. Li, J. Baeyens, P. Qin, A Particle-Driven, Ultrafast-Cured Strategy for Tuning the Network Cavity Size of Membranes with Outstanding Pervaporation Performance, ACS Appl Mater Interfaces 12(28) (2020) 31887-31895. https://doi.org/10.1021/acsami.0c05859.
[22] E. Ismail, N.H. Lazim, A. Nakata, A. Iwasawa, R. Yamanaka, I. Ichinose, Plasma-induced Interfacial Crosslinking of Liquid Polydimethylsiloxane Films and Their Organic Solvent Permeation Performance, Chem. Lett. 49(11) (2020) 1286-1290. https://doi.org/10.1246/cl.200504.

[23] S.M. Jordan, W.J. Koros, Permeability of pure and mixed gases in silicone rubber at elevated pressures, J. Polym. Sci. Part B Polym. Phys. 28(6) (1990) 795–809. https://doi.org/10.1002/polb.1990.090280602.

[24] R.D. Raharjo, B.D. Freeman, D.R. Paul, G.C. Sarti, E.S. Sanders, Pure and mixed gas CH_4 and *n*-C_4H_{10} permeability and diffusivity in poly(dimethylsiloxane), J. Memb. Sci. 306(1-2) (2007) 75–92. https://doi.org/10.1016/j.memsci.2007.08.014.

[25] L. Liu, E.S. Sanders, J.R. Johnson, O. Karvan, S. Kulkarni, D.J. Hasse, W.J. Koros, Influence of membrane skin morphology on CO_2/N_2 separation at sub-ambient temperatures, J. Memb. Sci. 446 (2013) 433–439. https://doi.org/10.1016/j.memsci.2013.06.001.

[26] G. Wulff, Fourty years of molecular imprinting in synthetic polymers: origin, features and perspectives, Microchim. Acta. 180 (2013) 1359–1370. https://doi.org/10.1007/s00604-013-0992-9.

[27] L. Chen, X. Wang, W. Lu, X. Wu, J. Li, Molecular imprinting: perspectives and applications, Chem. Soc. Rev. 45 (2016) 2137–2211. https://doi.org/10.1039/C6CS00061D.

[28] V. Arrighi, S. Gagliardi, A.C. Dagger, J.A. Semlyen, J.S. Higgins, M.J. Shenton, Conformation of cyclics and linear chain polymers in bulk by SANS, Macromolecules. 37(21) (2004) 8057–8065. https://doi.org/10.1021/ma049565w.

[29] J.S. Higgins, K. Dodgson, J.A. Semlyen, Studies of cyclic and linear poly(dimethyl siloxanes): 3. Neutron scattering measurements of the dimensions of ring and chain polymers, Polymer. 20(5) (1979) 553–558. https://doi.org/10.1016/0032-3861(79)90164-2.

[30] W.H. Briscoe, Polymers and Nanoscience, in: Colloid. Found. Nanosci., Elsevier, 2014: pp. 107–133. https://doi.org/10.1016/B978-0-444-59541-6.00005-9.

[31] P.G. de Gennes, Scaling Concepts in Polymer Physics, Cornell University Press, 1979.

[32] N. Stafie, D.F. Stamatialis, M. Wessling, Effect of PDMS cross-linking degree on the permeation performance of PAN/PDMS composite nanofiltration membranes, Sep. Purif. Technol. 45 (2005) 220–231. https://doi.org/10.1016/j.seppur.2005.04.001.

[33] B. Xu, J. Wu, G.B. McKenna, Mechanical and swelling behaviors of end-linked PDMS Rubber and randomly cross-linked polyisoprene, Macromolecules. 46 (2013) 2015–2022. https://doi.org/10.1021/ma302335u.

[34] A.M. Kansara, V.K. Aswal, P.S. Singh, Preparation and characterization of new poly(dimethylsiloxane) membrane series via a ‘cross-linking’ reaction using monomolecular trichloro(alkyl)silane of different alkyl chain and type, RSC Adv. 5(16) (2015) 51608–51620. https://doi.org/10.1039/C5RA06433C.

[35] G.L. Jadav, V.K. Aswal, P.S. Singh, *In-situ* preparation of polydimethylsiloxane membrane with long hydrophobic alkyl chain for application in separation of dissolved volatile organics from wastewater, J. Memb. Sci. 492 (2015) 95–106. https://doi.org/10.1016/j.memsci.2015.05.050.

[36] W. Ogieglo, H. van der Werf, K. Tempelman, H. Wormeester, M. Wessling, A. Nijmeijer, N.E. Benes, *n*-Hexane induced swelling of thin PDMS films under non-equilibrium nanofiltration permeation conditions, resolved by spectroscopic ellipsometry, J. Memb. Sci. 431 (2013) 233–243. https://doi.org/10.1016/j.memsci.2012.12.045.

[37] S.K. Patel, S. Malone, C. Cohen, J.R. Gillmor, R.H. Colby, Elastic modulus and equilibrium swelling of poly(dimethylsiloxane) networks, Macromolecules. 25(29) (1992) 5241–5251. https://doi.org/10.1021/ma00046a021.

[38] E.J. Kappert, M.J.T. Raaijmakers, K. Tempelman, F.P. Cuperus, W. Ogieglo, N.E. Benes, Swelling of 9 polymers commonly employed for solvent-resistant nanofiltration membranes: A comprehensive dataset, J. Memb. Sci. 569 (2019) 177–199. https://doi.org/10.1016/j.memsci.2018.09.059.

[39] S. Postel, C. Schneider, M. Wessling, Solvent dependent solute solubility governs retention in silicone based organic solvent nanofiltration, J. Memb. Sci. 497 (2016) 47–54. https://doi.org/10.1016/j.memsci.2015.09.014.

[40] F. Horkay, M. Zrinyi, E. Geissler, A.M. Hecht, P. Pruvost, Effect of neutral silica particles on the macroscopic swelling and elastic properties of polydimethyl siloxane networks, Polymer. 32(5) (1991) 835–839. https://doi.org/10.1016/0032-3861(91)90507-F.

[41] S.J. Lue, J.S. Ou, C.H. Kuo, H.Y. Chen, T.H. Yang, Pervaporative separation of azeotropic methanol/toluene mixtures in polyurethane–poly(dimethylsiloxane) (PU–PDMS) blend membranes: Correlation with sorption and diffusion behaviors in a binary solution system, J. Memb. Sci. 347(1-2) (2010) 108–115. https://doi.org/10.1016/j.memsci.2009.10.012.

[42] E. Favre, Swelling of crosslinked polydimethylsiloxane networks by pure solvents: Influence of temperature, Eur. Polym. J. 32(10) (1996) 1183–1188. https://doi.org/10.1016/S0014-3057(96)00062-6.

[43] E. Favre, Q.T. Nguyen, D. Sacco, A. Moncuy, R. Clement, Multicomponent polymer/solvents equilibria: an evaluation of Flory-Huggins theory for crosslinked PDMS networks swelled by binary mixtures, Chem. Eng. Commun. 140(1) (1995) 193–205. https://doi.org/10.1080/00986449608936463.

[44] N. Schuld, B.A. Wolf, Solvent quality as reflected in concentration- and temperature-dependent Flory-Huggins interaction parameters, J. Polym. Sci. Part B Polym. Phys. 39(6) (2001) 651–662. https://doi.org/10.1002/1099-0488(20010315)39:6<651::AID-POLB1039>3.0.CO;2-1.

[45] A. Muramoto, Studies on the Interaction Parameter in Polysiloxane Solutions, Polym. J. 1 (1970) 450–456. https://doi.org/10.1295/polymj.1.450.

[46] Y. Zhao, B.E. Eichinger, Study of solvent effects on the dilation modulus of poly(dimethylsiloxane), Macromolecules. 25(25) (1992) 6988–6995. https://doi.org/10.1021/ma00051a041.

[47] Y. Hu, X. Chen, G.M. Whitesides, J.J. Vlassak, Z. Suo, Indentation of polydimethylsiloxane submerged in organic solvents, J. Mater. Res. 26(6) (2011) 785–795. https://doi.org/10.1557/jmr.2010.35.
[48] N.A. Neuburger, B.E. Eichinger, Critical experimental test of the Flory-Rehner theory of swelling, Macromolecules. 21(10) (1988) 3060–3070. https://doi.org/10.1021/ma00188a026.
[49] G. Cocchi, M.G. De Angelis, F. Doghieri, Solubility and diffusivity of liquids for food and pharmaceutical applications in crosslinked polydimethylsiloxane (PDMS) films: I. Experimental data on pure organic components and vegetable oil, J. Memb. Sci. 492 (2015) 600–611. https://doi.org/10.1016/j.memsci.2015.04.063.
[50] S.P. Malone, C. Vosburgh, C. Cohen, Validity of the swelling method for the determination of the interaction parameter, Polymer. 34(24) (1993) 5149–5153. https://doi.org/10.1016/0032-3861(93)90261-8.
[51] W. Chassé, M. Lang, J.U. Sommer, K. Saalwächter, Cross-link density estimation of PDMS networks with precise consideration of networks defects, Macromolecules. 45(2) (2012) 899–912. https://doi.org/10.1021/ma202030z.
[52] T. Shiomi, K. Kuroki, A. Kobayashi, H. Nikaido, M. Yokoyama, Y. Tezuka, K. Imai, Dependence of swelling degree on solvent composition of two-component copolymer networks in mixed solvents, Polymer. 36(12) (1995) 2443–2449. https://doi.org/10.1016/0032-3861(95)97346-H.
[53] H. Yang, Q.T. Nguyen, Y. Ding, Y. Long, Z. Ping, Investigation of poly(dimethyl siloxane) (PDMS)–solvent interactions by DSC, J. Memb. Sci. 164(1-2) (2000) 37–43. https://doi.org/10.1016/S0376-7388(99)00187-8.
[54] J.B. Ott, J.R. Goates, (Solid + liquid) phase equilibria in binary mixtures containing benzene, a cycloalkane, an *n*-alkane, or tetrachloromethane An equation for representing (solid + liquid) phase equilibria, J. Chem. Thermodyn. 15(3) (1983) 267–278. https://doi.org/10.1016/0021-9614(83)90119-2.
[55] E.S. Domalski, E.D. Hearing, Heat capacities and entropies of organic compounds in the condensed phase. Volume III, J. Phys. Chem. Ref. Data. 25(1) (1996) 1–525. https://doi.org/10.1063/1.555985.
[56] H. Pan, J.A. Ritter, P.B. Balbuena, Examination of the approximations used in determining the isosteric heat of adsorption from the Clausius−Clapeyron equation, Langmuir. 14(21) (1998) 6323–6327. https://doi.org/10.1021/la9803373.
[57] K.M. Watson, Thermodynamics of the liquid state, Ind. Eng. Chem. 35(4) (1943) 398–406. https://doi.org/10.1021/ie50400a004.

[58] Y. Lai, Y. Hu, Probing the swelling-dependent mechanical and transport properties of polyacrylamide hydrogels through AFM-based dynamic nanoindentation, Soft Matter. 14 (2018) 2619–2627. https://doi.org/10.1039/C7SM02351K.
[59] S. Kitagawa, R. Kitaura, S. Noro, Functional porous coordination polymers, Angew. Chemie Int. Ed. 43(18) (2004) 2334–2375. https://doi.org/10.1002/anie.200300610.
[60] R. Kitaura, K. Seki, G. Akiyama, S. Kitagawa, Porous coordination-polymer crystals with gated channels specific for supercritical gases, Angew. Chemie Int. Ed. 42(4) (2003) 428–431. https://doi.org/10.1002/anie.200390130.
[61] R. Matsuda, R. Kitaura, S. Kitagawa, Y. Kubota, R.V. Belosludov, T.C. Kobayashi, H. Sakamoto, T. Chiba, M. Takata, Y. Kawazoe, Y. Mita, Highly controlled acetylene accommodation in a metal-organic microporous material, Nature. 436 (2005) 238–241. https://doi.org/10.1038/nature03852.
[62] P.J. Flory, J. Rehner, Statistical mechanics of cross-linked polymer networks II. Swelling, J. Chem. Phys. 11 (1943) 521–526. https://doi.org/10.1063/1.1723792.
[63] W.R. Vieth, P.M. Tam, A.S. Michaels, Dual sorption mechanisms in glassy polystyrene, J. Colloid Interface Sci. 22(4) (1966) 360–370. https://doi.org/10.1016/0021-9797(66)90016-6.

FIGURES

[COLOR] Figure 1. Preparation of PDMS rubbers and a schematic of the PDMS dispersions with different concentrations. The sample names are shown in the yellow box.

[COLOR] Figure 2. Presumed crosslinking structures of PDMS_0 (left) and PDMS_h5 with solvent molecules (right).

[COLOR] Figure 3. (a) Stress–strain curves for PDMS_h1, PDMS_h2, PDMS_h3, PDMS_h4, and PDMS_h5. The inset is the stress–strain curves for PDMS_0 and PDMS_h1. (b) Pictures of PDMS_0 and PDMS_h5 immediately before breaking and illustrations of their crosslinked polymer chains.

[COLOR] Figure 4. (a) Degree of swelling of PDMS_0, PDMS_h1, PDMS_h2, PDMS_h3, PDMS_h4 and PDMS_h5 rubbers in different hexane–ethanol mixtures. Swelling weights were measured using sealed containers to reduce the experimental error. (b) Volume increase of PDMS_0 and PDMS_h5 by hexane.

[COLOR] Figure 5. (a) Flory–Huggins' ΔH_{mix} (■) and $T\Delta S_{\mathrm{mix}}$ (♦) values of hexane/PDMS mixtures, and ΔH_{mix} (■) and $T\Delta S_{\mathrm{mix}}$ (♦) values of ethanol–PDMS mixtures at 298 K. (b) ΔG_{mix} of hexane–PDMS (●) and ethanol–PDMS (●) systems. (c) Illustration of the fluctuation of PDMS chains and their retention of hexane.

[COLOR] Figure 6. (a) Optical microscope images of PDMS_0 and PDMS_de4 powders prepared by cryogenic grinding. (b) Sorption isotherms of PDMS_0 (●), PDMS_de0.5 (●), and PDMS_de4 (●) at 298 K. (c) Sorption isotherms of PDMS_0 and PDMS_de4 at 195 K. (d) Comparison of the sorption isotherms of PDMS_de4 at 298 and 195 K. The *x*-axis is shown as the absolute pressure. The inset shows magnified plots in the low-pressure range.

[COLOR] Figure 7. (a) Comparison of the condensation heat (ΔH_{c}) and the sorption heat (ΔH_{sp}) of PDMS_0 (●) and PDMS_de4 (●) calculated by the Clausius–Clapeyron equation at 298 and 195 K. (b) The energy level diagrams for hexane sorption in PDMS_de4 at 298 and 195 K. ΔH_{mix}: mixing enthalpy change of hexane and PDMS; Expansion: energy loss by volume expansion of PDMS rubber; Stabilization: decrease in total energy mainly due to entropy change.

[COLOR] Figure 8. The changes in (a) elastic modulus, (b) Poisson's ratio, (c) bulk modulus, and (d) energy loss due to volume expansion with increasing sorption amount of decane at 298 K. PDMS rubbers: PDMS_0 (●) and PDMS_de4 (●). (e) The relationship between storage modulus and temperature for PDMS_0 and PDMS_de4 in the dried state. (f) Energy loss at 195 K for PDMS_0 and PDMS_de4. The insets in (a), (c), (d), and (f) are the magnified figures for PDMS_de4.

[COLOR] Figure 9. Comparison of hexane sorption isotherms of activated carbon [11] at 283 K and PDMS_de4 at 195 K, and the advantages of soft PDMS rubbers that exhibit the swelling memory effect.

TABLES

Table 1. Composition of reaction mixture, degree of overlapping concentration, and material properties of the obtained PDMS rubbers.

655 **Table 2.** Preparation conditions for PDMS rubbers, along with their dodecane content and DSC data.
656